Supporting Information

Low-dimensional magnetism in calcium nitridonickelate(II) Ca$_2$NiN$_2$

Simon D. Kloß*, J. Paul Attfield*

University of Edinburgh, Centre for Science at Extreme Conditions and School of Chemistry,

Edinburgh EH9 3FD, UK.

Table of Contents

1. Methods

Preparation of Ca_2NiN_2. Ca_2NiN_2 was prepared following Equation 1 from Ca_3N_2 (99.9 %, AlfaAesar), Ni powder (Fluka, carbonyl Ni) and NaN_3 (99.99%, Sigma-Aldrich) at 900 °C and 8 GPa achieved with a multianvil 1000 t large-volume hydraulic press (Voggenreither, Mainleus, Germany). At static pressure, the temperature was increased over 150 min after which a 300 min dwell and 60 min cooling phase followed. The starting materials were ground under inert conditions (<1 ppm H_2O, O_2) and filled into a Cu-capsule (0.025 mm thickness, 99.999 %, Puratronic®, AlfaAesar) before transferring into the 18/11 sized MgO-octahedron (Ceramic Substrates & Components, Isle of Wight, U.K.) employing an h-BN crucible (Henze, Kempten, Germany). Resistance heating was done via a double-layered graphite furnace (Schunk Kohlenstofftechnik GmbH, Zolling, Germany) and the octahedron was shielded from the heat via a ZrO_2 sleeve (Cesima Ceramics, Wust-Fischbeck, Germany). Details of the assembly can be found in the literature.[1] The reaction product was recovered from the octahedron under inert conditions.

Powder diffraction. PXRD data were collected in Transmission/Debye-Scherrer geometry with a Stadi P diffractometer (Stoe & CIE, Darmstadt, Germanx) equipped with a Mythen 1K detector (Dectris, Baden, Switzerland) and employing Cu-$K_{\alpha 1}$ radiation monochromatized with a Ge(111) single crystal. Samples were sealed in glass capillaries (Hilgenberg, Malsfeld, Germany) with 0.3 mm diameter and 0.01 mm wall thickness. The data were analyzed with Topas6 (Bruker, Billerica, MA, USA) and the crystal structure visualized with VESTA.[2] Powder data were analyzed by initial indexing using the single-value decomposition (SVD) method, Pawley extraction of reflection intensities, and structure solution using the charge-flipping algorithm with tangent formula as implemented in Topas6.[3–5]

Details of the Rietveld refinement are in Table 1. Deposition number CSD-2096979 contains the supplementary crystallographic data for this paper. These data are provided free of charge by the joint Cambridge Crystallographic Data Centre and Fachinformationszentrum Karlsruhe Access Structures service www.ccdc.cam.ac.uk/structures.

Temperature dependent PXRD data were collected in the range of 20–1000°C in steps of 20 K using a Stadi P diffractometer with Mo-$K_{\alpha 1}$ radiation and a position-sensitive image-plate detector. The sample was loaded under Ar in a 0.5 mm quartz capillary (Hilgenberg,

Malsfeld, Germany) and sealed with grease to retain the inert atmosphere during the measurement. Data was analyzed with the WinXPOW software and Rietveld analysis performed with Topas6.[6] The measurement was conducted in flowing N_2 with 30 min/step and soon after the capillary break the sample was cooled to room temperature, which might explain why metallic Ni instead of NiO was formed.

EDX spectroscopy. EDX spectra of the microcrystalline sample were obtained with a EVO-Ma 10 (Zeiss, Oberkochen, Germany) scanning electron microscope. Selected particles were placed on adhesive carbon tape under inert gas atmosphere and quickly inserted into the microscope to avoid sample decomposition. The EVO-Ma 10 was equipped with a field emission gun run at 15 keV and a Bruker X-Flash 410-M detector. Data were analysed with the QUANTAX 200 software package. Oxygen content was not taken into account owing to the short exposure in air and consequential hydrolysis. Samples were not sputtered owing to the hydrolysis.

Magnetometry.

Magnetization curves $M(H,T)$ were recorded with a Quantum Design Physical Properties Measurement System (PPMS) on powdered samples of Ca_2NiN_2, which were packed into polyethylene capsules and sealed with glue to prevent decomposition. Isothermal magnetization curves in the range of ± 50 kOe were recorded at temperatures of 300 and 2.5 K, while the temperature dependent susceptibility was obtained at 30 kOe in the range of 2.5 to 300 K. The obtained magnetizations were corrected for the diamagnetic contribution of the capsule.

The susceptibility was fit with a combination of a Bonner-Fisher-function χ_{BF} and a Curie-function to account for an impurity tail. Bonner-Fisher-function χ_{BF} was expressed as:

$$\chi_{BF} = \frac{N_A \cdot \mu_{eff}^2}{3 \cdot k_B \cdot T} \frac{0.25 + 0.149445x + 0.30094x^2}{1 + 1.9862x + 0.68854x^2 + 6.0626x^3} \text{ with } x = \frac{|J|}{k_B \cdot T}$$

The fitted values were $\mu_{eff} = 2.19$ μ_B for the paramagnetic moment and exchange constant $J = -157$ K, as described in the main text.
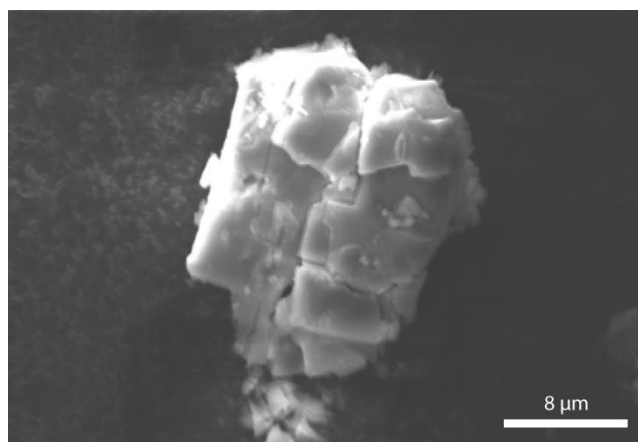
2. Scanning electron microscopy

Figure S1: SEM image of Ca_2NiN_2 crystallites showing smooth surfaces on which energy dispersive X-ray (EDX) spectroscopy was carried out.

Table S1: Results of EDX analysis carried out on Ca_2NiN_2. Evenly distributed Na at the 5 at-% level is omitted from the analysis for clarity.

Datapoint	N content / at-%	Ca content / at-%	Ni content / at-%
1	50.3	34.3	15.4
2	43.8	38.9	17.3
3	34.9	44.4	20.7
4	45.4	37.0	17.7
5	41.7	39.9	18.4
6	44.8	38.7	16.5
7	32.6	46.0	21.4
8	39.2	41.5	19.3
9	35.8	44.4	19.8
10	42.5	39.6	17.9
11	37.8	40.3	22.0
12	45.9	34.2	19.9
13	40.7	41.0	18.3
14	35.5	44.4	20.1
15	37.7	42.5	19.8
16	34.5	46.0	19.5
17	44.5	38.2	17.3
18	45.6	38.3	16.1
Mean / at-%	40.7	40.5	18.7
ESD / at-%	4.8	3.5	1.8
Normalized on Ca	2.0	2.0	0.9
ESD normalized on Ca	0.2	0.2	0.1

3. Structure analysis

Table S2: Crystallographic data and atom positions of Ca_2NiN_2.

Crystal data	
Sum formula	Ca_2NiN_2
Formula mass, g·mol^{-1}	166.86
Crystal system	Tetragonal
Space group	$I4/mmm$ (no. 139)
Cell parameters, Å	$a = 3.57206(2)$
	$c = 12.19453(10)$
Volume, Å^3	155.719(5)
Z	2
$F(000)$	164
Calc. density, g·cm^{-3}	3.561
Absorption coef., μ, mm^{-1}	35.585
Data collection	
Radiation	Laboratory X-ray, Cu-K$_{\alpha 1}$
Temperature, K	297(2)
d-range, Å	17.66–0.88
No. of datapoints	7705
No. of reflections	51
Refinement	
No. of parameters	12
R_{Bragg}	1.99
R_p, R_{wp}	3.72, 5.04
GoF	1.31

Atom positions and displacement parameters						
Atom	Wyckoff	x	y	z	Occupancy	U_{eq} / Å^2
Ni1	2a	0	0	0	1	0.0204(4)
Ca1	4e	0	0	0.34681(5)	1	0.0174(2)
N1	4e	0	0	0.1433(2)	1	0.0205(8)

Table S3: Anisotropic displacement parameters of Ca_2NiN_2.

Atom	U_{11} / Å^2	U_{22} / Å^2	U_{33} / Å^2	U_{23} / Å^2	U_{13} / Å^2	U_{12} / Å^2
Ni1	0.0208(5)	0.0208(5)	0.0196(8)	0	0	0
Ca1	0.0195(3)	0.0195(3)	0.0132(6)	0	0	0
N1	0.0148(10)	0.0148(10)	0.032(2)	0	0	0

Table S4: Bond valence sum calculations of Ca_2NiN_2. Bond valence parameters reported by O'Keeffe were used for Ni-N ($r_0 = 1.75$ Å) and Ca-N ($r_0 = 2.14$ Å) bond pairs along with empirical constant $b = 0.37$. A bond distance cutoff of 4 Å was used.[7]

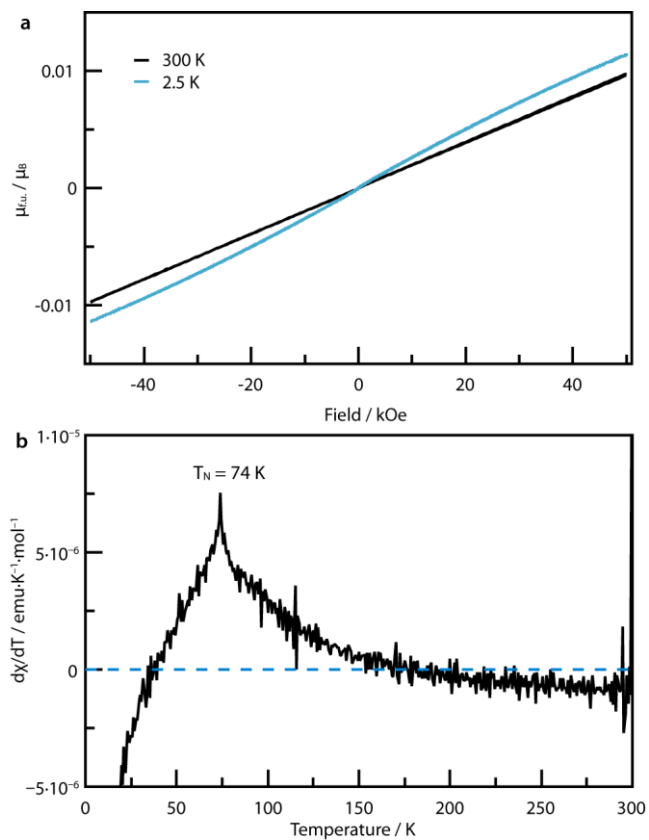| Cation-Anion Pair	Bond Distance / Å	v_{ij}
Ni1–N1	1.748	1.005
Ni1–N1	1.748	1.005
Ni1–N1	3.9766	0.002
Ni1–N1	3.9766	0.002
Ni1–N1	3.9766	0.002
Ni1–N1	3.9766	0.002
Ni1–N1	3.9766	0.002
Ni1–N1	3.9766	0.002
Ni1–N1	3.9766	0.002
Ni1–N1	3.9766	0.002
$V_{Ni,N}$		**2.030**
Ca1–N1	2.5287	0.350
Ca1–N1	2.5287	0.350
Ca1–N1	2.5287	0.350
Ca1–N1	2.5287	0.350
Ca1–N1	2.482	0.397
$V_{Ca,N}$		**1.796**

4. Magnetization

Figure S2: a Field-dependent magnetization at 300 and 2.5 K showing linear field dependence typical for an antiferromagnet **b** dχ/dT plot highlighting a possible long-range antiferromagnetic transition at $T_N = 74$ K.

5. References

1   H. Huppertz, *Z. Kristallogr. 2004*, **219**, 330.

2   K. Momma and F. Izumi, *J. Appl. Crystallogr. 2011*, **44**, 1272.

3   A. A. Coelho and *J. Appl. Crystallogr. 2003*, **36**, 86–95.

4   G. S. Pawley, *J. Appl. Crystallogr. 1981*, **14**, 357.

5   A. A. Coelho, *Acta Crystallogr. Sect. A: Found. Crystallogr. 2007*, **63**, 400.

6   STOE&Cie GmbH, *WinXPOW*, Darmstadt, *2007*.

7   N. E. Brese and M. O'Keeffe, *Acta Crystallogr. Sect. B 1991*, **47**, 192.